

Nos résultats montrent que la liaison Ru—Cl(1) = 2,317 (7) Å n'est pas affectée par la formation des liaisons Ru—O—Ru puisqu'on mesure la même longueur que dans le composé $K_2[RuCl_6]$ [2,318 (2) Å]. Toutes les autres liaisons sont plus longues [Ru—Cl(2) = 2,362 (2) Å]. La distance de l'atome de chlore Cl(1) au plan défini par les quatre atomes de chlore Cl(2), Cl(2ⁱ), Cl(2ⁱⁱ), Cl(2ⁱⁱⁱ) est plus courte [2,196 (2) Å] que dans l'ion $[RuCl_6]^{2-}$ [2,318 (2) Å]. En outre la plus courte distance mesurée entre deux atomes de chlore [Cl(1)···Cl(2) = 3,223 (6) Å] est comparable à celle observée dans $K_2[RuCl_6]$ [3,279 (3) Å].

Morrow (1962) a montré que le composé $K_4[Re_2Cl_{10}O].H_2O$ était isotype de $K_4[Ru_2Cl_{10}O].H_2O$. Cet auteur ayant opéré de la même manière que Mathieson, Mellor & Stephenson (1952), nos résultats permettent de penser que pour ce composé il n'y a pas non plus de molécule d'eau et que sa formule est $K_4[Re_2Cl_{10}O]$.

Tebbe & Schnering (1973) ont trouvé pour le composé $Cs_4[Os_2Cl_{10}O]$ une géométrie comparable bien que le groupe d'espace (*Pcab*) n'impose pas la symétrie D_{4h} pour l'ion $[Os_2Cl_{10}O]^{4-}$. L'homologue de la liaison Ru—Cl(1) a une longueur de 2,433 (7) Å et on mesure pour les homologues des liaisons Ru—Cl(2), Ru—Cl(2ⁱ), Ru—Cl(2ⁱⁱ), Ru—Cl(2ⁱⁱⁱ): 2,375 (6), 2,370 (6), 2,367 (6), 2,371 (6) Å soit en moyenne Os—Cl(2)_{moyen} = 2,371 (6) Å. On constate donc une déformation différente pour les liaisons ruthénium—chlore et osmium—chlore:

$$Ru-Cl(1) = 2,317 (7) \text{ \AA} \quad Os-Cl(1) = 2,433 (7) \text{ \AA}$$

$$Ru-Cl(2) = 2,362 (2) \quad Os-Cl(2)_{\text{moyen}} = 2,371 (6)$$

Outre la précision apportée aux paramètres structuraux nous avons donc pu montrer que les sels de potassium des ions $[Ru_2Cl_{10}O]^{4-}$ et $[Re_2Cl_{10}O]^{4-}$

cristallisent sans molécule d'eau. Les différences constatées entre le sel de césium de l'ion $[Os_2Cl_{10}O]^{4-}$ et le sel de potassium de l'ion $[Ru_2Cl_{10}O]^{4-}$ rendent intéressante une étude comparative des sels alcalins des chlorocomplexes des métaux qui forment des ions du type $[M_2Cl_{10}O]^{4-}$.

Les calculs ont été effectués sur ordinateur IBM 370-168 à Orsay (CIRCE) par l'intermédiaire du Terminal de l'Institut de Recherches sur la Catalyse de Lyon et à l'aide d'une bibliothèque de programmes classiques organisée par H. Loiseleur au laboratoire de Chimie Analytique II (Quaglieri, Loiseleur & Thomas, 1972).

Références

- ADAMS, C. S. & MELLOR, D. P. (1952). *Aust. J. Sci. Res.* **5**, 577–578.
- ANTHONY, U. & LUCCHESI, A. (1899). *Gazz. Chim. Ital.* pp. 312–318.
- BOL'SHAKOV, K. A., SINITSYN, N. M. & BORISOV, V. V. (1972). *Russ. J. Inorg. Chem.* **17**, 1731–1734.
- CHARONNAT, R. (1931). *Ann. Chim. Phys.* **16**, 5–121.
- CLARK, R. J. H., FRANKS, M. L. & TURTLE, P. C. (1977). *J. Am. Chem. Soc.* **99**, 2473–2480.
- International Tables for X-ray Crystallography* (1974). Tome IV. Birmingham: Kynoch Press.
- MATHIESON, A. McL., MELLOR, D. P. & STEPHENSON, N. C. (1952). *Acta Cryst.* **5**, 185–186.
- MORROW, J. C. (1962). *Acta Cryst.* **15**, 851–855.
- QUAGLIERI, P., LOISELEUR, H. & THOMAS, G. (1972). *Acta Cryst.* **B28**, 2583–2590.
- REMY, H. & LUHRS, A. (1928). *Chem. Ber.* **61**(B), 917–925.
- SAN FILIPPO, J., GRAYSON, R. L. & SNIADACH, H. J. (1976). *Inorg. Chem.* **15**, 269–274.
- TEBBE, K. F. & SCHNERING, H. (1973). *Z. Anorg. Allg. Chem.* **396**, 66–80.
- WOODHEAD, J. L. & FLETCHER, J. M. (1962). Atomic Energy Research Establishment, R 4123, Harwell, England.

Acta Cryst. (1979). **B35**, 561–564

Structure Image of $Yb_3Fe_4O_{10}$ by a 1 MV High-Resolution Electron Microscope

BY YOSHIQ MATSUI, KATSUO KATO, NOBORU KIMIZUKA AND SHIGEO HORIUCHI

National Institute for Researches in Inorganic Materials, Sakura-mura, Niihari-gun, Ibaraki, Japan 330-31

(Received 19 July 1978; accepted 8 November 1978)

Abstract

1 MV high-resolution electron microscope images of a crystal of $Yb_3Fe_4O_{10}$ have been taken to elucidate its crystal structure. The structure consists of the alternate stacking of three different types of layers. Positions of individual Yb and Fe ions are resolved within each

layer as giving spots having dark and gray contrasts respectively. The crystal is often intergrown on a unit-cell scale with other phases, which belong to the same series of homologous compounds in an Fe— Fe_2O_3 — Yb_2O_3 system.

A series of homologous compounds, $(\text{YbFeO}_3)_n \cdot \text{FeO}$ ($n = 1$ to 4), have been prepared in an $\text{Fe}-\text{Fe}_2\text{O}_3-\text{Yb}_2\text{O}_3$ system (Kimizuka & Katsura, 1975; Kimizuka, Kato, Shindo, Kawada & Katsura, 1976). The crystal structures of YbFe_2O_4 ($n = 1$) and $\text{Yb}_2\text{Fe}_3\text{O}_7$ ($n = 2$) have been determined by Kato, Kawada, Kimizuka & Katsura (1975) and Kato, Kawada, Kimizuka, Shindo & Katsura (1976). The structure of YbFe_2O_4 ($R\bar{3}m$, $a = 3.455$, $c = 25.05$ Å) is described by the alternate stacking of two types of layers, having the components $\text{Yb}^{3+}\text{O}_{3/2}(U)$ and $\text{Fe}^{2+}\text{Fe}^{3+}\text{O}_{5/2}(W)$, in the $[001]$ direction. Each Yb ion occupies the center of a slightly deformed octahedron formed by six O atoms, while both Fe^{2+} and Fe^{3+} ions occupy the special equivalent positions in the trigonal bipyramids formed by five O atoms. In $\text{Yb}_2\text{Fe}_3\text{O}_7$ ($P6_3/mmc$, $a = 3.476$, $c = 28.43$ Å) a third type of layer, $\text{Fe}^{3+}\text{O}_{3/2}(V)$, occurs in the stacking sequence of layers. Fe^{3+} ions in this layer also occupy the center of the trigonal bipyramids.

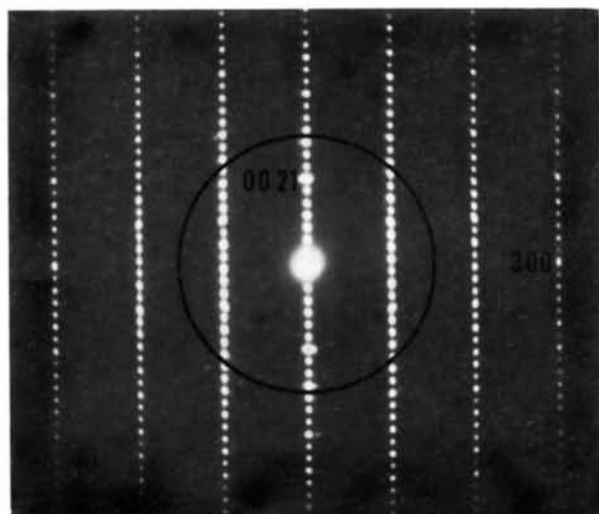
The structures of $\text{Yb}_3\text{Fe}_4\text{O}_{10}$ ($n = 3$) and $\text{Yb}_4\text{Fe}_5\text{O}_{13}$ ($n = 4$) were inferred on the basis of the crystal-chemical considerations, and the X-ray powder diffraction patterns of these crystals were indexed from the hypothetical structures (Kimizuka *et al.*, 1976). The X-ray refinement of the structure of $\text{Yb}_3\text{Fe}_4\text{O}_{10}$ was, however, unsuccessful (the best R value was 0.27 and the weighted R value was 0.17), probably because of the poor crystallization of the specimen used for the intensity measurement.

A 1 MV high-resolution electron microscope (Hitachi-1250 type) was recently constructed based on the theory of electron optics (Scherzer, 1949; Horiuchi & Matsui, 1974). The resolution limit of the microscope is 2.0 Å when a goniometer stage is used (Horiuchi, Matsui & Bando, 1976). Images taken at about 1000 Å underfocus reflect the projected potential of the crystals more precisely than do those for 100 kV class microscopes, because a greater number of diffracted waves can contribute to imaging with increase of the accelerating voltage. In the case of $4\text{Nb}_2\text{O}_5 \cdot 9\text{WO}_3$, for example, small dark dots were identified as individual cation sites according to the computer simulation of image contrast (Horiuchi, Muramatsu & Matsui, 1978). In order to test the hypothetical structure model for a crystal of $\text{Yb}_3\text{Fe}_4\text{O}_{10}$, its structure images were observed by the 1 MV microscope in the present study.

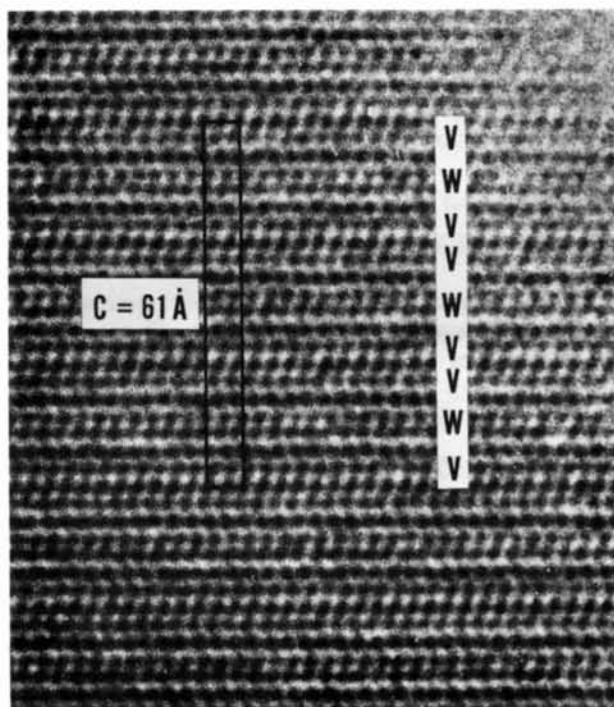
The crystals prepared by Kimizuka *et al.* (1976) were ground in CCl_4 in an agate mortar. The fragments were collected on a holey carbon supporting film and observed in the 1 MV electron microscope. The procedure for taking the images was that reported previously (Horiuchi *et al.*, 1976).

We examined the diffraction patterns showing various reciprocal-lattice sections of the crystal of $\text{Yb}_3\text{Fe}_4\text{O}_{10}$. For the hexagonal lattice with $a = 3.5$ Å and $c = 61$ Å, the reflections appear only when $-h + k + l = 3n$, indicating that the crystal has rhombohedral

symmetry. Fig. 1(a) shows an electron diffraction pattern taken with the incident beam normal to the (110) plane. The circle drawn in the figure indicates the size and the position of the objective aperture employed



(a)



(b)

Fig. 1. (a) Electron diffraction pattern of a $\text{Yb}_3\text{Fe}_4\text{O}_{10}$ crystal taken with the incident beam normal to the (110) plane. The circle shows the size of the objective aperture used for taking the image in (b). (b) Structure image of $\text{Yb}_3\text{Fe}_4\text{O}_{10}$ by a 1 MV high-resolution electron microscope. Each site of Yb and Fe is resolved as a dark and a gray spot respectively. The lines of the former correspond to $\text{YbO}_{3/2}(U)$ type layers, while those of the latter correspond to $\text{FeO}_{3/2}(V)$ or $\text{Fe}_2\text{O}_{5/2}(W)$ type layers.

for the present 1 MV electron microscope. The size corresponds to 0.5 \AA^{-1} in reciprocal space and enables about 50 diffracted waves to contribute to imaging.

Fig. 1(b) shows a 1 MV structure image of a crystal of $\text{Yb}_3\text{Fe}_4\text{O}_{10}$ obtained at about 1000 \AA underfocus. According to our previous experiences mentioned above, dark and gray spots are interpreted to represent the positions of Yb and Fe ions respectively. It is evident that the crystal is composed of three different regularly alternating types of layers which include Yb, single Fe and double Fe respectively. Taking into account the trigonal symmetry, it can be reasonably assumed from the observed positions of the cations that, within each layer, they occupy the special positions in the hexagonal lattice: $0,0,z$, $\frac{1}{3},\frac{2}{3},z$ and $\frac{2}{3},\frac{1}{3},z$; the x and y coordinates of the cations can be determined from a single photograph (Fig. 1b). The three layers can then correspond to the U , V and W layers mentioned above. The positions of the O atoms can be assigned so that octahedra or trigonal bipyramids are formed around each cation. The crystal structure thus obtained is shown schematically in Fig. 2. The space

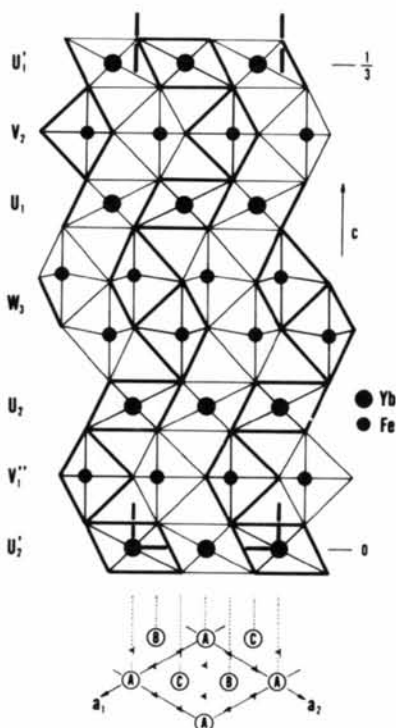
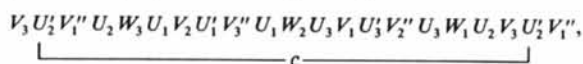


Fig. 2. Crystal structure model of $\text{Yb}_3\text{Fe}_4\text{O}_{10}$. Only one third of the unit cell is shown. The remaining two thirds are derived by the threefold screw axes shown in the lower figure. Large and small dark circles represent Yb and Fe ions respectively. YbO_6 octahedra and FeO_5 trigonal bipyramids are represented schematically. The darker and lighter polyhedra are centered on the two levels perpendicular to the $[110]$ direction and are 1.75 \AA apart.

group is $R\bar{3}m$. The structure model can be expressed symbolically by the stacking of layers:



where subscripts indicate the differences in x, y coordinates. U and U' are symmetrically independent, while V and V'' are related by the inversion operation. This layer sequence agrees with that previously proposed by Kimizuka *et al.* (1976).

Fig. 3 was obtained from another grain with an incident beam normal to the (100) plane. Only 00/ reflections can contribute to imaging in this orientation and, therefore, one-dimensional lattice fringes are obtained. The layers U , V and W are, however, mutually distinguished as those with dark, gray and double-gray lines respectively. The $\text{Yb}_3\text{Fe}_4\text{O}_{10}$ phase is formed in a very limited region in this case. Three V -type layers are often inserted between the W -type layers, corresponding to the formation of $\text{Yb}_4\text{Fe}_5\text{O}_{13}$ ($n = 4$), as shown in the figure. In other regions five or six

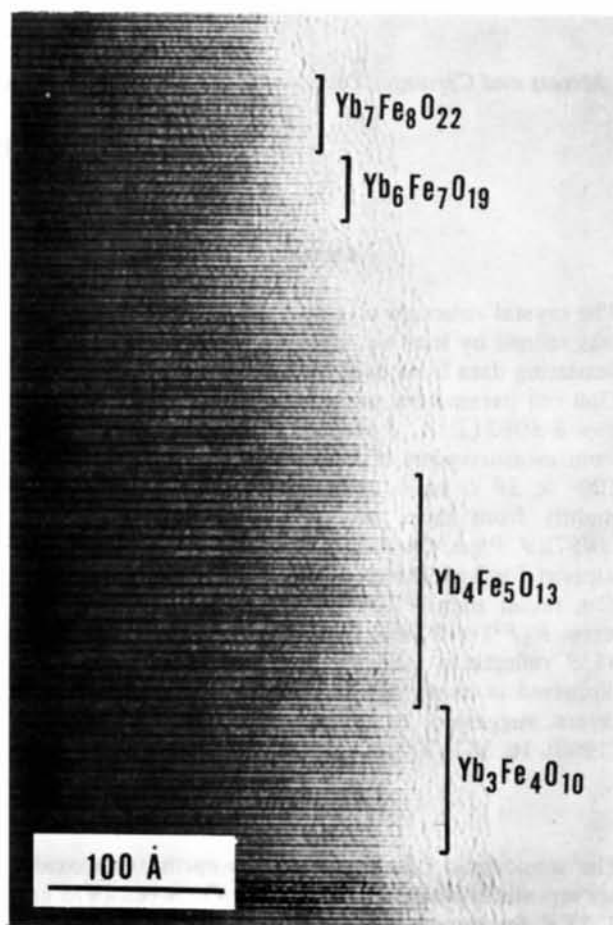


Fig. 3. Lattice image taken with the incident beam normal to the (100) plane. $\text{Yb}_3\text{Fe}_4\text{O}_{10}$ ($n = 3$) and $\text{Yb}_4\text{Fe}_5\text{O}_{13}$ ($n = 4$) are observed almost equally. $\text{Yb}_6\text{Fe}_7\text{O}_{19}$ ($n = 6$) and $\text{Yb}_7\text{Fe}_8\text{O}_{22}$ ($n = 7$) are locally intergrown in fine scales.

V -type layers are adjoined to the W -type layers. These may correspond to $\text{Yb}_6\text{Fe}_7\text{O}_{19}$ ($n = 6$) or $\text{Yb}_7\text{Fe}_8\text{O}_{22}$ ($n = 7$). A similar intergrowth of these homologous phases was often observed in other grains. It may then be reasonable to consider that such frequent intergrowths have made the accurate X-ray structure analysis of $\text{Yb}_3\text{Fe}_4\text{O}_{10}$ difficult.

The authors wish to express their deep gratitude to Dr Y. Bando for valuable discussions and to Mr Y. Sekikawa for help in the experiment.

References

HORIUCHI, S. & MATSUI, Y. (1974). *Philos. Mag.* **30**, 777–787.

HORIUCHI, S., MATSUI, Y. & BANDO, Y. (1976). *Jpn. J. Appl. Phys.* **15**, 2483–2484.

HORIUCHI, S., MURAMATSU, K. & MATSUI, Y. (1978). *Acta Cryst.* **A34**, 939–946.

KATO, K., KAWADA, I., KIMIZUKA, N. & KATSURA, T. (1975). *Z. Kristallogr.* **141**, 314–320.

KATO, K., KAWADA, I., KIMIZUKA, N., SHINDO, I. & KATSURA, T. (1976). *Z. Kristallogr.* **143**, 278–284.

KIMIZUKA, N., KATO, K., SHINDO, I., KAWADA, I. & KATSURA, T. (1976). *Acta Cryst.* **B32**, 1620–1621.

KIMIZUKA, N. & KATSURA, T. (1975). *J. Solid State Chem.* **15**, 151–157.

SCHERZER, O. (1949). *J. Appl. Phys.* **20**, 20–29.

Acta Cryst. (1979). **B35**, 564–569

A Refinement of the Crystal Structure of Monoclinic Europium Sesquioxide*

BY HARRY L. YAKEL

Metals and Ceramics Division, Oak Ridge National Laboratory, PO Box X, Oak Ridge, Tennessee 37830, USA

(Received 6 September 1978; accepted 20 November 1978)

Abstract

The crystal structure of monoclinic europia ($B\text{-Eu}_2\text{O}_3$) was refined by least-squares analyses of Mo $K\alpha$ X-ray scattering data from over 5000 independent reflections. Unit-cell parameters, $a = 14.1105$ (2), $b = 3.6021$ (1), $c = 8.8080$ (2) Å, $\beta = 100.037$ (1)°, were computed from measurements of Bragg angles of reflections with $100^\circ < 2\theta < 163^\circ$. Atom position parameters differ slightly from those reported for $B\text{-Sm}_2\text{O}_3$ [Cromer (1957). *J. Phys. Chem.* **61**, 753–755]. There is no clear support for hypotheses that the space group is $C2$ or Cm , rather than $C2/m$. Final measures of agreement were: $R(F^2) = 0.041$, $R_w = 0.065$, and $\sigma_1 = 1.24$ for 4538 reflections with $F_o^2 > \sigma(F_o^2)$. The structure is discussed in terms of the tetrahedrally linked $(MO)_n^{2+}$ layers suggested by Caro [*J. Less-Common Met.* (1968). **16**, 367–377].

Introduction

The monoclinic (B) forms of rare-earth sesquioxides are reportedly stable at temperatures between 1273 and 2273 K for elements near the middle of the lanthanide

series (Glushkova, 1965). In a phase diagram they occur between the low-temperature cubic (C) and high-temperature hexagonal (A) phases. A crystal structure for a $B\text{-Ln}_2\text{O}_3$ phase was first presented by Cromer (1957), who studied a fragment of $B\text{-Sm}_2\text{O}_3$ from a boule melted at 3273–3773 K in an oxyacetylene flame. Atoms were all located in the mirrors of space group $C2/m$; the structure determination and refinement were performed with a few hundred $h0l$ data uncorrected for absorption.

In view of the renewed interest in structural factors affecting the stability and transformation rates of rare-earth oxides, and because the precision of Cromer's results might be improved by detailed analysis of more extensive data, a study of the crystal structure of $B\text{-Eu}_2\text{O}_3$ was undertaken.

Experimental

Growth of high-purity $B\text{-Eu}_2\text{O}_3$ crystals by convective mass transport from molten NaF has been described by Bennett, Finch, Yakel, Brynstad & Clark (1977). Crystals from this process were preferred for the structural study because (a) the growth temperature (1423–1473 K) was in the B -phase stability region, (b) the growth could be carried out in dry (<5 p.p.m. H_2O)

* Research sponsored by the Materials Sciences Division, US Department of Energy, under contract W-7405-eng-26 with the Union Carbide Corporation.